

# Selective Blockade of the Ubiquitous Checkpoint Receptor CD47 Is Enabled by Dual-Targeting Bispecific Antibodies

Elie Dheilly,<sup>1,2</sup> Valéry Moine,<sup>1,2</sup> Lucile Broyer,<sup>1</sup> Susana Salgado-Pires,<sup>1</sup> Zoë Johnson,<sup>1</sup> Anne Papaioannou,<sup>1</sup> Laura Cons,<sup>1</sup> Sébastien Calloud,<sup>1</sup> Stefano Majocchi,<sup>1</sup> Robert Nelson,<sup>1</sup> François Rousseau,<sup>1,3</sup> Walter Ferlin,<sup>1</sup> Marie Kosco-Vilbois,<sup>1</sup> Nicolas Fischer,<sup>1</sup> and Krzysztof Masternak<sup>1</sup>

<sup>1</sup>Novimmune SA, 14 chemin des Aulx, 1228 Plan-les-Ouates, Switzerland

**CD47 is a ubiquitously expressed immune checkpoint receptor that is often upregulated in cancer. CD47 interacts with its counter-receptor SIRP $\alpha$  on macrophages and other myeloid cells to inhibit cancer cell phagocytosis and drive immune evasion. To overcome tolerability and “antigen sink” issues arising from widespread CD47 expression, we generated dual-targeting bispecific antibodies that selectively block the CD47-SIRP $\alpha$  interaction on malignant cells expressing a specific tumor-associated antigen; e.g., CD19 or mesothelin. These bispecific  $\kappa\lambda$  bodies are fully human, native IgG1 molecules, combining tumor targeting and selective CD47 blockade with immune activating mechanisms mediated by the Fc portion of the antibody. CD47-neutralizing  $\kappa\lambda$  bodies efficiently kill cancer cells in vitro and in vivo but interact only weakly with healthy cells expressing physiological levels of CD47. Accordingly, a  $\kappa\lambda$  body administered to non-human primates showed a typical IgG pharmacokinetic profile and was well tolerated. Importantly,  $\kappa\lambda$  bodies preserve their tumoricidal capabilities in the presence of a CD47 antigen sink. Thus, dual-targeting  $\kappa\lambda$  bodies allow for efficacious yet safe targeting of CD47 in cancer. Such a bispecific design could be applied to limit the extent of neutralization of other ubiquitously expressed therapeutic targets.**

## INTRODUCTION

Recent clinical success of monoclonal antibodies targeting T cell checkpoint pathways has spawned unprecedented enthusiasm about cancer immunotherapy as an effective means of curing cancer or, at least, taming cancer to transform it into a chronic illness.<sup>1,2</sup> However, the final success of immunotherapy will ultimately depend on combined mobilization of multiple arms of the immune system, including innate immune cells that sit at the interface between cancer and its microenvironment, and act both as effectors and coordinators of anti-tumor and tumor-promoting immune responses.<sup>3–6</sup> Mononuclear phagocytes, such as macrophages, are key players shaping the immune environment of the tumor. Not surprisingly, cancer cells have evolved mechanisms to evade recognition and immune attack by these cells. A commonly used stratagem is to hijack CD47, a ubiq-

uitous innate immune checkpoint receptor used to control homeostatic phagocytosis.<sup>7–10</sup>

CD47 inhibits phagocytosis by engaging signal regulatory protein alpha (SIRP $\alpha$ ) on the effector cell, which induces a de-phosphorylation cascade paralyzing the actomyosin machinery needed for the engulfment process.<sup>7,8,11</sup> The “don’t eat me” signal conveyed by the CD47-SIRP $\alpha$  interaction efficiently offsets potent “eat me” signals from phagocytosis-activating receptors such as Fc-gamma receptors, complement receptors, or low-density lipoprotein receptor-related protein 1 (LRP1).<sup>12,13</sup> Cancer cells upregulating CD47 trick the immune system to prevent it from mounting effective antitumor responses.<sup>9,10,14</sup> CD47 is overexpressed on a majority of hematological and solid tumors, with particularly high levels on cancer stem cells (CSCs),<sup>9,15–19</sup> and high CD47 levels are generally correlated with poor survival.<sup>9,10,17,19–24</sup> In preclinical experiments, CD47 blockade increased phagocytosis of tumor cells in vitro and potentiated anti-tumor therapies in numerous human xenograft models.<sup>9,10,20,21,23–28</sup> In addition to stimulating cancer cell phagocytosis, CD47 blockade was shown to support other anti-tumor mechanisms, such as enhancement of antibody-dependent cell-mediated cytotoxicity (ADCC),<sup>26</sup> direct induction of apoptosis of cancer cells by CD47 cross-linking,<sup>18,29–31</sup> induction of differentiation of CSCs, and inhibition of tumorigenicity.<sup>19,28,32,33</sup> CD47 neutralization was also recently shown to promote the development of anti-tumor adaptive T cell responses,<sup>34–37</sup> possibly as a consequence of increased tumor cell uptake by professional antigen-presenting cells and enhanced antigen cross-presentation.<sup>14,38</sup> Hence, there is a strong rationale for therapeutic targeting of CD47, and numerous strategies are currently being pursued toward this goal. The most advanced are two anti-CD47

Received 5 July 2016; accepted 4 November 2016;  
<http://dx.doi.org/10.1016/j.ymthe.2016.11.006>.

<sup>2</sup>These authors contributed equally to this work.

<sup>3</sup>Present address: Glenmark Pharmaceuticals SA, 5 chemin de la Combeta, 2300 La Chaux de Fonds, Switzerland

**Correspondence:** Krzysztof Masternak, Novimmune SA, 14 chemin des Aulx, 1228 Plan-les-Ouates, Switzerland.

**E-mail:** [kmasternak@novimmune.com](mailto:kmasternak@novimmune.com)

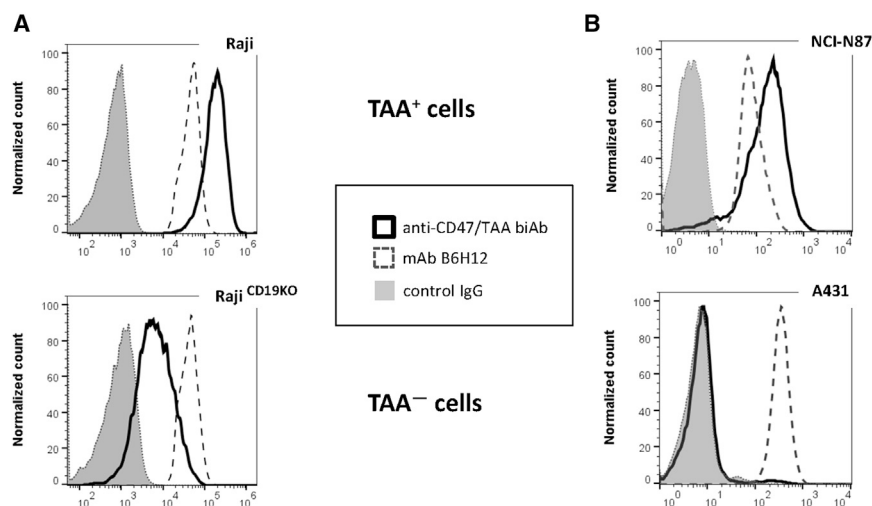


**Figure 1. Binding Selectivity of Dual-Targeting Bispecific Antibodies**

Binding of the CD47/TAA bispecific antibody to TAA-positive and TAA-negative cells was analyzed by flow cytometry. Histogram plots show the staining of TAA-positive, CFSE-labeled cells (top) and TAA-negative unlabeled cells (bottom) mixed at a 1:1 ratio and co-incubated with CD47/TAA bispecific antibody (empty profiles, black line), anti-CD47 mAb B6H12 (empty profiles, dashed line), or negative IgG controls (gray shaded profiles). (A) CD47/CD19 bispecific antibody binding to double-positive Raji cells and CD19-negative Raji<sup>CD19KO</sup> cells. (B) CD47/mesothelin bispecific antibody binding to mesothelin-positive HPAC cells and mesothelin-negative A431 cells.

blocking monoclonal antibodies and a receptor fusion protein (SIRP $\alpha$ -Fc) that recently entered human trials (NCT02678338, NCT02641002, NCT02367196, and NCT02663518). However, because CD47 is ubiquitously expressed, the efficacy and the safety of these CD47 blocking strategies may be negatively affected by a large antigen sink represented by healthy cells.<sup>39</sup> A proposed solution is to target the receptor of CD47 instead (i.e., SIRP $\alpha$ ), which has a more restricted expression pattern.<sup>26,40</sup>

Yet another alternative would be to use dual-targeting bispecific antibodies (biAbs) with the aim of limiting CD47 neutralization to cancer cells. Because of physical association of two antibody arms with different antigen specificities, biAbs offer new mechanisms of action, not supported by traditional monoclonal antibodies (mAbs) or antibody mixes, paving the way to new therapeutic opportunities.<sup>41–43</sup> For instance, dual-targeting biAbs can concurrently engage two different antigens on the cell surface, which stabilizes antibody binding to double-positive cells through an avidity effect,<sup>44</sup> and such a design can be used for selective blockade of CD47 on cancer cells expressing a specific tumor antigen. Indeed, two recently published papers describe rituximab-based tetravalent anti-CD47/CD20 bispecific constructs with selectivity to CD20-positive B lymphoma cells and potent tumoricidal capabilities.<sup>45,46</sup> Here we present two examples of CD47-neutralizing dual-targeting biAbs. The first of these biAbs targets CD19, a B cell marker broadly expressed in B cell leukemias and lymphomas. The second one is specific to mesothelin (MSLN), an antigen overexpressed in multiple solid tumors, with particularly high prevalence in pancreatic and ovarian carcinomas, and in malignant pleural mesothelioma.<sup>47</sup> These anti-CD47/CD19 and anti-CD47/MSLN biAbs are unmodified human immunoglobulin G1s (IgG1s). As such, they combine tumor targeting and CD47 blockade with immune-activating mechanisms mediated by the constant Fc portion, enabling efficient antibody Fc-mediated killing.<sup>48–50</sup> We demonstrate that these dual-targeting biAbs selectively block CD47 on double-positive tumor cells to induce potent macrophage-mediated antibody-dependent cellular phagocytosis (ADCP). Tumor tar-

geting is precise, efficacious, and safe because these CD47-neutralizing biAbs bind poorly to normal healthy cells and are not subject to CD47-mediated clearance in vivo, and their tumoricidal capabilities are not affected by antigen sink.

## RESULTS

### Anti-CD47/TAA Bispecific Antibodies Selectively Target Double-Positive Tumor Cells

We have recently reported the development of a novel biAb format, the  $\kappa\lambda$  body.<sup>51</sup>  $\kappa\lambda$  bodies are native, fully human IgG1s composed of a common heavy chain and two different light chains, one kappa and one lambda. The CD47-neutralizing biAbs used in this study are  $\kappa\lambda$  bodies having one antibody arm (kappa) specific for CD47 and a second arm (lambda) specific to a tumor-associated antigen (TAA), either CD19 or mesothelin (Figure S1). The high-affinity anti-TAA arm serves to tether the antibody to double-positive (CD47+/TAA+) cells. On the other hand, the anti-CD47 antibody arm is the “effector arm” of the biAb, as its primary function is to promote phagocytosis by CD47 blockade. Because it interacts weakly with CD47 and does not have a sufficiently high affinity to sustain efficient binding to TAA-negative cells, the function of the anti-CD47 antibody arm is strictly dependent on dual targeting; i.e., co-engagement of CD47 and the TAA on the surface of double-positive cells.

To demonstrate binding selectivity, we incubated anti-CD47/TAA biAbs in a 1:1 mixture of double-positive (target) cells and single-positive (CD47-positive/TAA-negative, non-target) cells and then analyzed for antibody binding by flow cytometry (Figures 1A and 1B). The anti-CD47/CD19 biAb bound potently to CD19-positive Burkitt’s lymphoma Raji cells (Raji) but only weakly to CD19-negative mutant cells (Raji<sup>CD19KO</sup>) (Figure 1A). Likewise, the anti-CD47/MSLN biAb bound selectively to double-positive NCI-N87 gastric carcinoma cells but not to mesothelin-negative A431 epidermoid carcinoma cells (Figure 1B). In contrast, binding selectivity was not observed with B6H12, a mouse anti-human CD47-neutralizing monoclonal antibody widely used in CD47 research (Figures 1A and 1B).<sup>52</sup> These results show that dual-targeting biAbs are able

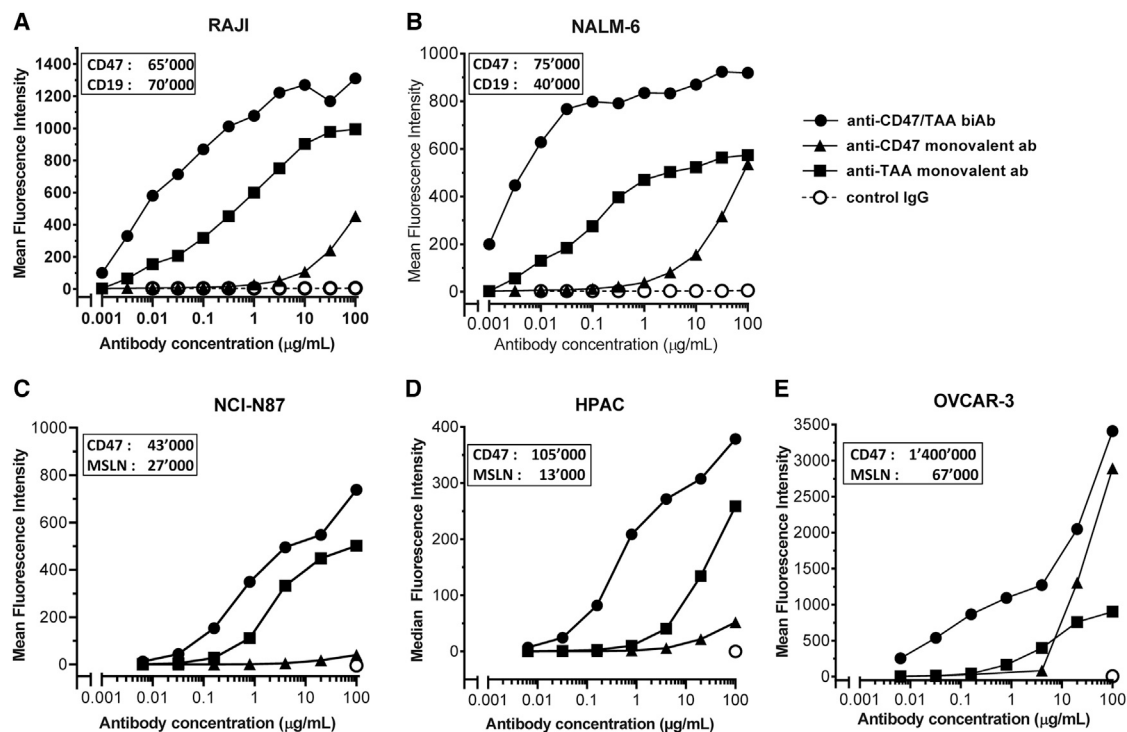


**Figure 2. Contribution of Anti-CD47 and Anti-TAA Bispecific Antibody Arms to Binding Potency**

Shown is binding of bispecific versus monovalent antibodies to double-positive cells. (A and B) Dose response with the anti-CD47/CD19 antibody and the corresponding monovalent controls binding to Raji (A) and NALM-6 (B) cells. (C–E) Dose response with the anti-CD47/mesothelin antibody and the corresponding monovalent controls binding to NCI-N87 (C), HPAC (D), and OVCAR-3 cells (E). Insets show antigen cell surface density as the number of molecules per cell. Representative experiments are shown.

to differentiate between target and non-target cells, implying that binding selectivity is driven by the anti-TAA antibody arm. To confirm the respective contributions of individual antibody arms, we generated control monovalent antibodies (that is,  $\kappa\lambda$  bodies in which one of the antibody arms was replaced by a neutral, non-binding arm) and assessed their binding to double-positive cells by flow cytometry (Figures 2A–2E). Binding of the anti-CD47/CD19 biAb and its monovalent counterparts was tested with Raji and NALM-6 cells, a B cell acute lymphoblastic leukemia (B-ALL) cell line (Figures 2A and 2B). Binding of anti-CD47/anti-MSLN antibodies was assessed with three epithelial tumor cell lines expressing varying levels of CD47. In addition to the gastric carcinoma NCI-N87 cells, a pancreatic adenocarcinoma cell line, HPAC, and an ovarian carcinoma cell line, OVCAR-3, were also tested (Figures 2C–2E, see insets for cell surface antigen expression levels). Monovalent anti-TAA antibodies bound strongly to target cells, in contrast to monovalent anti-CD47 antibodies, which displayed either weak binding (Figures 2A, 2B, and 2E; Raji NALM-6 and OVCAR-3 cells) or no detectable binding (Figures 2C and 2D; NCI-N87 and HPAC cells). Overall, these results confirm the role of the anti-TAA arm for binding selectivity. The anti-CD47 arm contributes to the stabilization of antibody binding through avidity generated upon concurrent engagement of the two antigens on the cell surface, as revealed by the comparison of binding profiles generated with the biAbs and the corresponding monovalent

anti-TAA antibodies. Of note, elevated binding activity of the monovalent anti-CD47 antibody was observed with OVCAR-3 cells, which can be explained by particularly high levels of CD47 expression in this cell line (Figure 2E, inset).

We hypothesized that TAA co-engagement would result in increased CD47 blockade at the surface of target cells. To verify this assumption, we compared the activity of the anti-CD47/CD19 biAb and the corresponding monovalent anti-CD47 control in a SIRP $\alpha$  competitive binding assay. As expected, the biAb, but not the anti-CD47 monovalent antibody, potentially blocked the binding of soluble SIRP $\alpha$ -Fc to Raji and NALM-6 cells (Figure S2), thus confirming that co-engagement of the cognate TAA is required for efficient neutralization of CD47 on the surface of target cells.

#### Anti-CD47/TAA Bispecific Antibodies Induce Tumor Cell Killing In Vitro and In Vivo

Macrophage-mediated ADCP is a clinically relevant Fc-dependent effector mechanism of anti-cancer therapeutic antibodies,<sup>5,6,53</sup> and its efficacy is enhanced upon blocking the CD47 “don’t eat me” signal.<sup>9,10</sup> To test the efficacy of anti-CD47/TAA biAbs in ADCP, peripheral blood monocyte-derived macrophages were incubated with tumor cells in the presence of increasing antibody concentrations, and their phagocytic activity was assessed by three different

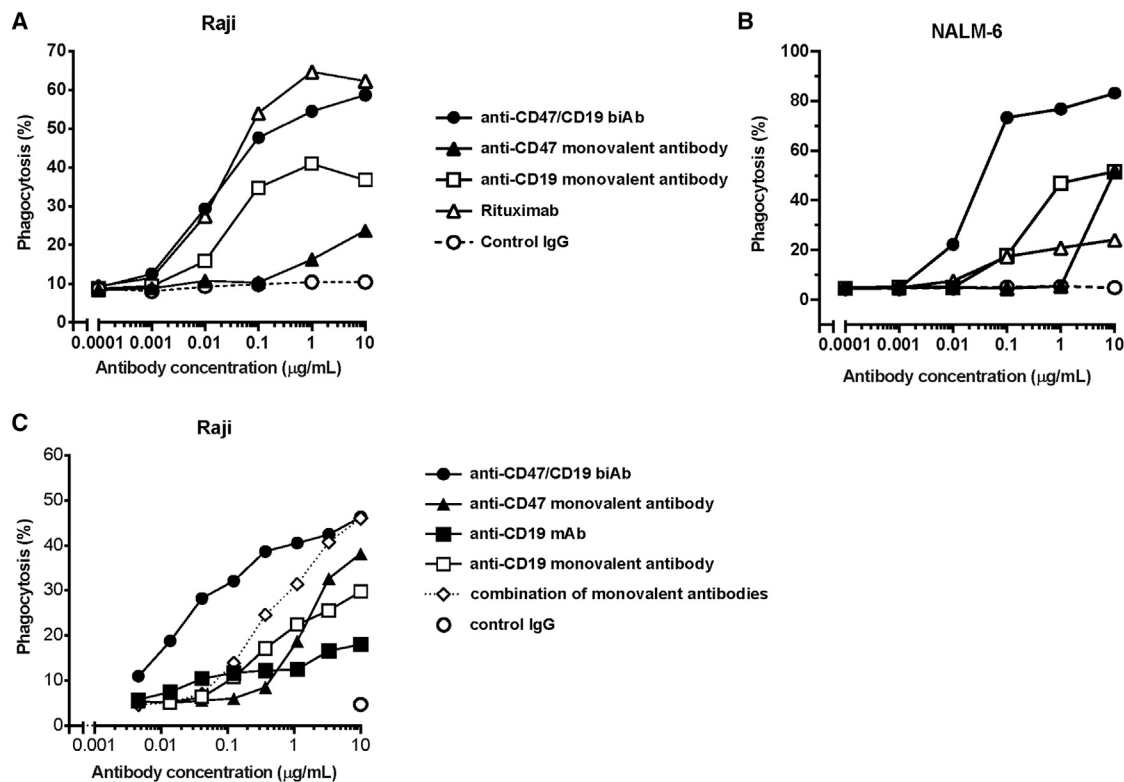


**Figure 3. Anti-CD47/CD19 BiAb-Mediated Phagocytosis**

Raji (A and C) and NALM-6 B cells (B) were incubated with donor-derived macrophages (E:T ratio 1:5) and increasing concentrations of the indicated antibodies. Phagocytosis was assessed by flow cytometry and is expressed as the percentage of macrophages that ingested at least one target cell. (A and B) Monovalent antibodies and the anti-CD20 mAb rituximab were tested for comparison. (C) Phagocytosis induced by individual monovalent antibodies, a 1/1 mixture thereof, and the anti-CD47/CD19 biAb. Data are representative of at least two independent experiments.

techniques: traditional flow cytometry (Figures 3 and 4; Figures S3 and S6), imaging flow cytometry (Figure S4), and microscopy-based cellular quantitative imaging (Figure S6). High levels of phagocytosis of Raji cells were induced by the anti-CD47/CD19 biAb, comparable with rituximab, reported to mediate potent ADCP with CD20-overexpressing cell lines (Figure 3A; Figure S4A).<sup>54</sup> In contrast, monovalent control antibodies elicited markedly lower levels of phagocytosis, in particular the anti-CD47 monovalent antibody (Figure 3A; Figure S3A). We therefore conclude that CD47-CD19 co-engagement at the surface of target cells is important for high ADCP activity and that CD19-negative cells should be much more resistant to phagocytosis induced by the anti-CD47/CD19 biAb compared with double-positive cells. An experiment comparing biAb-mediated phagocytosis of wild-type (double-positive) Raji cells with engineered Raji CD19 knockout cells supports this idea. Contrary to wild-type Raji cells, Raji<sup>CD19KO</sup> cells were not efficiently phagocytosed in the presence of the anti-CD47/CD19 biAb, at least not more efficiently than with the anti-CD47 monovalent antibody (Figure S3). Last but not least, we demonstrated that the anti-CD47/CD19 biAb was significantly more potent than a mixture of monovalent anti-CD47 and anti-CD19 antibodies, especially at lower antibody concentrations (Figure 3C). This experiment clearly shows the importance of the

physical association of the two antibody arms within a single molecule and of the resulting avidity effect generated upon concurrent binding of the two antibody arms to the target cell. The importance of avidity was further corroborated by ADCP experiments in which the biAb again showed to be more efficient than a mixture of monovalent antibodies (Figure S5). ADCP experiments were also performed with the B-ALL cell line NALM-6 (Figure 3B), confirming the importance of CD19 expression (and CD47-CD19 co-engagement) for efficient biAb-mediated phagocytosis. By the way, rituximab was inefficient with NALM-6 cells (Figure 3B; Figure S4B), which can be explained by low CD20 expression levels. The anti-CD47/MSLN biAb was tested in ADCP experiments using NCI-N87, HPAC, and OVCAR-3 target cells. The results of representative experiments are shown in Figure 4. To account for variance between peripheral blood monocyte-derived macrophages, we show additional ADCP experiments in Figure S6. In addition, Figures S6A–S6E show an experiment aimed at a comparative assessment of two different phagocytosis assay methods. In the first one, ADCP occurs in solution and is detected by flow cytometry as double-fluorescence events (this our classical way of assessing phagocytosis). The second method involves adherent macrophages and high-throughput cellular quantitative fluorescence microscopy. The three epithelial tumor cell lines used in ADCP

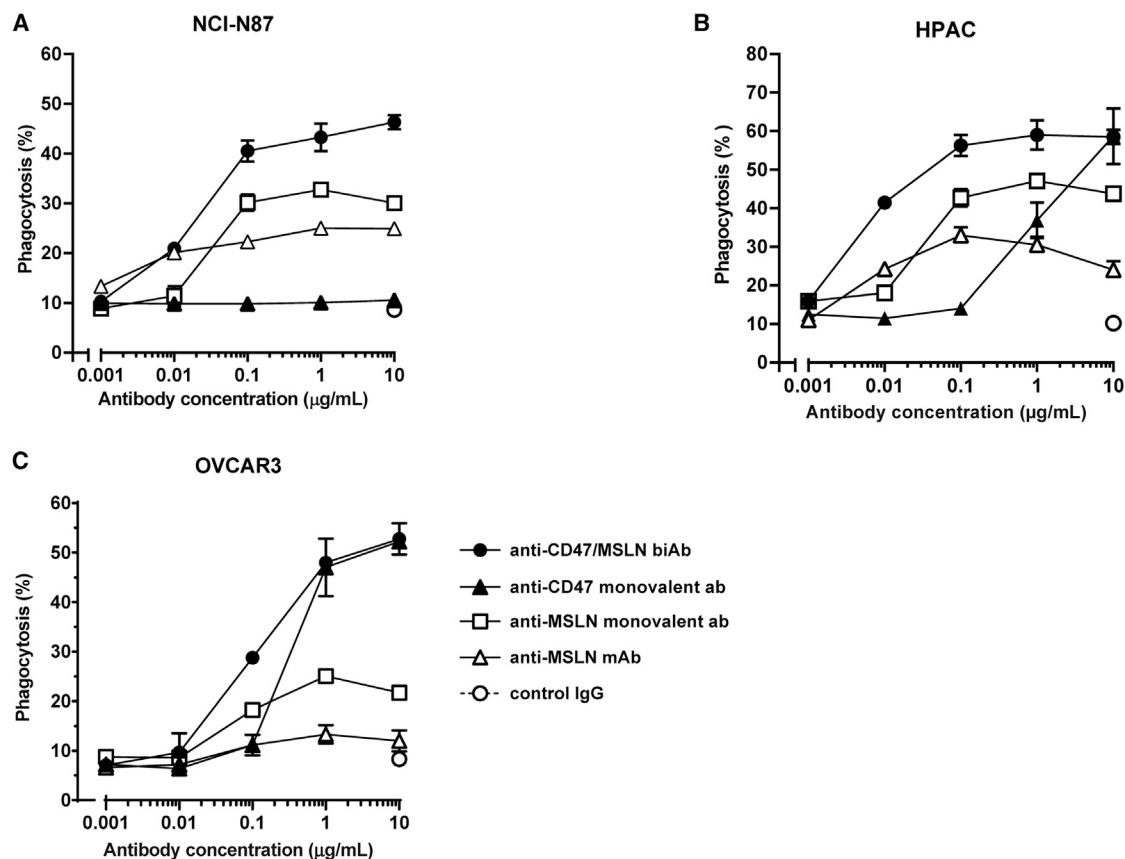


**Figure 4. Anti-CD47/Anti-MSLN Antibody-Mediated Phagocytosis**

NCI-N87 (A), HPAC (B), and OVCAR-3 (C) epithelial tumor cells were incubated with donor-derived macrophages (E:T ratio 3:1) and increasing concentrations of the indicated antibodies. Percent phagocytosis was defined as in Figure 3. Data are representative of at least two independent experiments.

experiments express quite varied levels of cell surface antigens, in particular of CD47 (see insets in Figures 2C–2E). Arguably, CD47 expression levels were the major factor influencing phagocytosis mediated by the anti-CD47 monovalent antibody. Although the biAb-mediated and the anti-MSLN antibody-mediated ADCP levels were consistent across the three cell lines, the efficacy of the monovalent anti-CD47 antibody varied appreciably. No phagocytosis was observed with NCI-N87 cells, which express “physiological” levels of CD47, around 20,000–40,000 copies of CD47 per cell (Figure 4; Figures S6A–S6D). In contrast, appreciable levels of phagocytosis were apparent with the two cell lines overexpressing CD47, HPAC, and OVCAR-3, expressing, respectively, 100,000 and 1,500,000 antigen copies per cell (Figure 4; Figures S6E and S6F). The ADCP efficacy of the anti-CD47 monovalent antibody was remarkably high with OVCAR-3 cells, showing that generous overexpression of CD47, as often found in cancer cells and CSCs, can compensate for the absence of matching levels of TAA on the cell surface. Overall, the experiments described above allow us to conclude that the neutralization of the “don’t eat me” signal plus an avid binding to target cells generated upon co-engagement of CD47 and the TAA translate into a synergistic enhancement of Fc-mediated tumor cell killing.

Finally, we tested the anti-CD47/CD19 biAb in a xenograft model with subcutaneous Raji tumors implanted in non-obese diabetic (NOD)/severe combined immunodeficiency (SCID) mice. In these in vivo experiments, we compared the efficacy of the biAb to two mAbs, a high-affinity anti-CD19 mAb (the mAb from which the anti-CD19 arm of the biAb was derived) and the CD47 blocking mAb B6H12. As described by others,<sup>21</sup> we observed a meaningful effect of B6H12 in this model. In contrast, the anti-CD19 mAb used as a single agent showed only marginal efficacy, if any, indicating that targeting CD19 is not sufficient to control tumor growth. On the other hand, the anti-CD47/CD19 biAb or the synergistic combination of B6H12 and the anti-CD19 mAb potently induced tumor regression (Figure 5). These results thus confirm that efficient tumor killing requires both CD47 neutralization and antibody Fc-mediated effector functions.<sup>21, 25</sup>

#### **Efficacy and Pharmacokinetics of the Anti-CD47/CD19 Bispecific Antibody Are Not Affected by Antigen Sink**

Abundant expression of target antigen in healthy tissue is a potential barrier to the development of therapeutic antibodies. This is particularly true with CD47, which is expressed on virtually every cell.

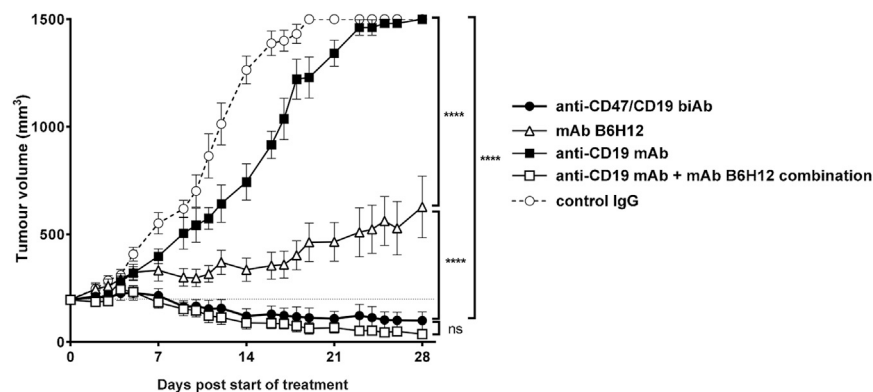


**Figure 5. Anti-CD47/CD19 Bispecific Antibody Effect on Tumor Growth In Vivo**

NOD/SCID mice transplanted subcutaneously with Raji cells were recruited to the experiment when the tumor volume reached about 200 mm<sup>3</sup>, divided into treatment groups (n = 10), and treated intraperitoneally (i.p.) with 400 μg of the indicated antibody or an antibody mix (400 μg + 400 μg) three times per week for 4 weeks. Tumor growth was measured daily and is shown as average tumor size per group ± SEM. Statistical significance was determined using one-way ANOVA on day 28. \*\*\*\*p < 0.0001; ns, not significant.

Hence, indiscriminate CD47 binding may result in decreased antibody bioavailability, rapid elimination because of antigen sink, as well as on-target toxicities. The anti-CD47/TAA dual-targeting biAbs were designed to bypass these limitations by enabling preferential targeting of TAA-positive tumor cells over TAA-negative healthy cells. To demonstrate hematological safety, we tested the binding of the anti-CD47/CD19 biAb to red blood cells (RBCs). RBCs express CD47 levels in the range of 20,000–25,000 antigen copies per cell<sup>55,56</sup> and represent the most abundant circulating population (around five billion RBCs per milliliter of blood). Whole-blood assays comparing binding of the anti-CD47/CD19 biAb to RBCs versus CD19-positive B cells showed strong staining of the latter (Figure 6A) but little, if any, staining of RBCs, even at the highest antibody concentrations (150 μg/mL; Figures 6B and 6C). To confirm our findings, we assessed the fraction of antibody bound to cells in the blood at equilibrium. For this, anti-CD47/CD19 biAbs were incubated with undiluted whole human blood followed by removal of the cellular fraction by centrifugation and then measurement of the antibody remaining in the plasma. In contrast to mAb B6H12, the anti-CD47/CD19 biAb plasma concentration was not diminished by adsorption to cells, thus confirming its low potential for interacting with human erythrocytes (Figure S7). Binding to other blood cell populations, such as neutrophils or platelets, was also weak, and the anti-CD47/CD19 biAb did not induce platelet activation or aggregation (Figure S8 and data not shown). Whole-blood binding experiments performed with the anti CD47/MSLN biAb showed an even weaker binding to human blood cells (data not shown), which is consistent with the lower affinity of its anti-CD47 arm compared with the anti-CD47/CD19 biAb.

We also assessed the effect of RBCs on the efficacy of ADCP. In these experiments, human erythrocytes were used as a proxy of antigen sink, mimicking diverse CD47-positive cell populations that can be found in the tumor microenvironment, the liver, or the lymphoid organs. As shown in Figure 6D, the presence of erythrocytes had no effect on the efficacy of the anti-CD47/CD19 biAb, but phagocytosis induced by mAb B6H12-hIgG1 (B6H12 bearing a human IgG1 Fc portion) was significantly decreased. A similar RBC-mediated inhibition of ADCP was also observed with native B6H12 (mouse IgG1) as well as with other anti-CD47 mAbs (data not shown), revealing an

effect of antigen sink on CD47 antibody function with potential relevance to in vivo efficacy.

The effect of ubiquitous CD47 expression on pharmacokinetic (PK) behavior of the anti-CD47/CD19 biAb was studied in non-human primates (NHPs). The anti-CD19 arm of the biAb is not cross-reactive with NHP CD19 orthologs. However, the anti-CD47 arm of the biAb has a similar affinity to human and cynomolgus antigens, as determined by surface plasmon resonance (data not shown), and the anti-CD47/CD19 biAb binds with comparable potency to human and cynomolgus blood cells (Figure S8). Consequently, the cynomolgus monkey is a relevant species for testing CD47-mediated drug clearance. We therefore performed a single-dose PK study in which the CD47/CD19 biAb was administered intravenously at two dose levels, 0.5 mg/kg and 10 mg/kg. There was no evidence of non-linear pharmacokinetic behavior at either dose level, suggesting that there was no target-mediated clearance of the anti-CD47/CD19 biAb (Figure 7; Table S1). The antibody was well tolerated; we did not observe any clinical symptoms, hematological toxicities (Figure S9), or macroscopic evidence of target organ toxicity attributable to the treatment.

## DISCUSSION

CD47, a checkpoint receptor and promoter of immune escape, is overexpressed in cancer and, thus, represents an attractive target for immunotherapeutic intervention. The other side of the coin is that CD47 is a universal marker of “self” in normal healthy tissue, regulating programmed cell removal by homeostatic phagocytosis. Moreover, CD47 is also involved in other, disparate physiological processes ranging from regulation of cardiovascular homeostasis, neuronal development, bone remodeling, and adaptive immunity to response to stress, stem cell renewal, cell adhesion, motility, proliferation, and survival (reviewed by Oldenberg,<sup>57</sup> Barclay and Van den Berg,<sup>58</sup> Sick et al.,<sup>59</sup> Soto-Pantoja et al.,<sup>60</sup> Sarfati et al.,<sup>61</sup> Murata et al.,<sup>62</sup> and Matozaki et al.<sup>63</sup>). Hence, therapeutic targeting of CD47 with agents blocking CD47 in an indiscriminate manner, such as anti-CD47 monoclonal antibodies, may not only be inefficient—because of antigen sink—but also potentially dangerous. As a matter of fact, CD47 blockers administered to rodents and NHPs were shown to induce hematotoxicity.<sup>10,20,25,39</sup> In particular,

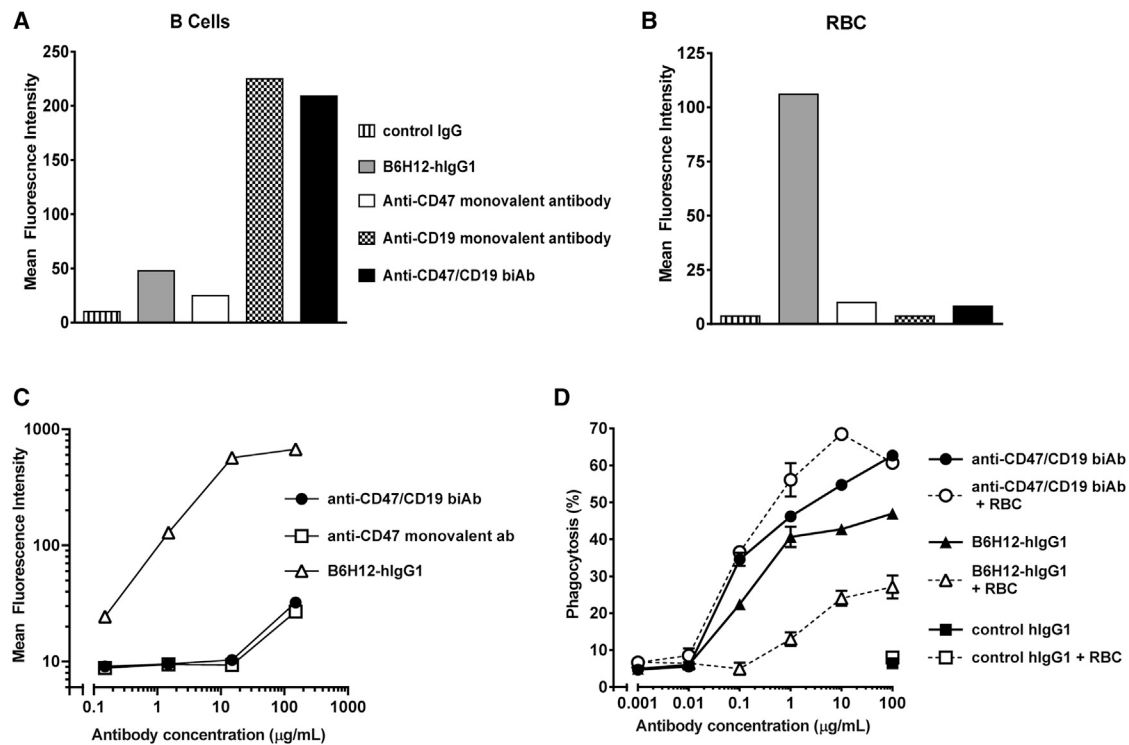


**Figure 6. Binding of Anti-CD47/CD19 Bispecific Antibody to Human RBCs and the Effect of Antigen Sink on ADCP Efficacy**

(A–C) Human whole-blood cytometry. Whole blood from a healthy donor was incubated with the indicated antibodies pre-labeled with a fluorescent anti human Fc detection reagent. Binding to CD20-positive B cells (A) or red blood cells stained with an anti-glycophorin A antibody (B and C) was assessed by three-color flow cytometry and is expressed as mean fluorescence intensity. Primary antibodies were tested at a concentration of 3 µg/mL (A and B) or in dose response (C). (D) ADCP of Raji cells was induced with anti-CD47/CD19 biAb or mAb B6H12-hlgG1 as described in Figure 3. The effect of CD47 antigen sink on antibody efficiency was assessed by including purified human RBCs (final concentration  $5 \times 10^8$  RBCs/mL) in the phagocytosis reaction. A representative experiment is shown.

poor tolerability was observed with anti-CD47 mAbs and a high-affinity SIRP $\alpha$  variant-Fc fusion protein bearing an immunologically active Fc portion, whereas effector-less CD47 blockers were shown to be relatively safe (Weiskopf et al.<sup>25</sup> and C.E. Pietsch et al., 2015, Cancer Res., abstract). This implies that clinically developable anti-CD47 mAbs and other general CD47 inhibitors should bear silenced or greatly attenuated Fc portions, if any. Such effector-less CD47 inhibitors block the “don’t eat me” signal and were shown to enhance tumor cell killing mediated by Fc $\gamma$ R-engaging tumor-specific mAbs,<sup>21,25,26</sup> but their intrinsic activity is limited or nil (Weiskopf et al.<sup>25</sup> and C.E. Pietsch et al., 2015, Cancer Res., abstract). Hence, the downside to the safety benefit of abrogating Fc effector functions is also the liability in terms of efficacy, relegating effector-less CD47 blockers to the role of discretionary adjuvants of therapeutic anti-tumor mAbs, which can be seen as a limitation from a drug developability standpoint.

Dual-targeting bispecific antibodies provide an all-in-one solution to this conundrum because they associate efficient tumor targeting, blockade of CD47, and potent Fc-dependent killing functions within a single antibody molecule. Antigen sink effects and the effect on normal tissue can be minimized by carefully tuning the affinity of

the anti-CD47 antibody arm in a way that provides for efficient tumor cell killing while avoiding collateral damage to healthy cells expressing physiological levels of CD47. The selectivity mediated by the anti-TAA arm of these bispecific molecules dramatically increases the safety margin of therapeutic CD47 targeting. As a consequence, anti-CD47/TAA biAbs can be safely endowed with an immunologically active Fc portion, thus arming them with autonomous Fc-mediated tumor cell killing capabilities. The two examples described in this publication demonstrate the feasibility of such a dual-targeting strategy. We show that these biAbs selectively bind double-positive tumor cells co-expressing CD47 and a TAA, CD19, or mesothelin. Using monovalent control antibodies, we also demonstrate that the binding selectivity of these biAbs is largely contingent on the anti-TAA antibody arm, whereas the anti-CD47 arm contributes to the stabilization of the interaction with the target cell through an avidity effect. Co-engagement of the TAA on tumor cells mediates efficient CD47 blockage and the disruption of the “don’t eat me” signal, which eventually translate into high levels of macrophage-mediated tumor cell killing. On the other hand, these anti-CD47/TAA biAbs interact poorly with normal healthy cells and are thus able to evade the negative effects of antigen sink on both antibody effector function and pharmacokinetics.

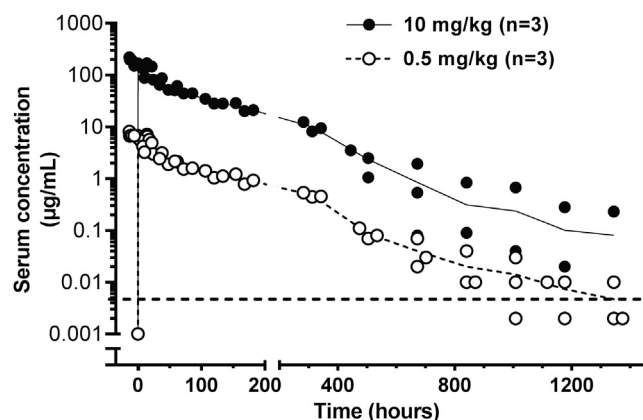


**Figure 7. Pharmacokinetics of the Anti-CD47/CD19 Bispecific Antibody in Cynomolgus Monkeys**

Serum concentration of the anti-CD47/CD19 bispecific antibody after single intravenous (i.v.) administration to cynomolgus monkeys in function of time. Two different doses of antibody were administered as an i.v. bolus injection, 0.5 mg/kg (dotted lines), and 10 mg/kg (solid lines);  $n = 3$  for each dose level. Serum concentrations of individual animals are shown.

To conclude, we prove here that dual-targeting biAbs are an efficient yet safe means of therapeutic neutralization of CD47 in cancer, adding an innovative and complementary anti-tumor mechanism to the existing immuno-oncology drug armamentarium. In more general terms, the biAbs described in this publication provide a proof of principle that could be exploited to therapeutically address other ubiquitously expressed antibody targets.

## MATERIALS AND METHODS

### Bispecific Antibodies

Fixed immunoglobulin heavy chain variable domain (VH) library construction, phage display selection and screening,  $\kappa\lambda$  body production, purification, and analytical characterization are described in detail by Fischer et al.<sup>51</sup>

### Cell Lines and Reagents

Human cancer cell lines were obtained from the ATCC. The Burkitt's lymphoma cell line Raji (CCL-86), B cell acute lymphoblastic leukemia cell line NALM-6 (ACC-128), acute T cell leukemia cell line Jurkat (TIB-152), ovary adenocarcinoma cell line OVCAR3 (HTB-161), and gastric carcinoma cell line NCI-N87 (CRL-5822) were cultured in RPMI 1640. The A-431 epidermoid carcinoma cell line (CRL-1555) was cultured in DMEM and the HPAC pancreatic adenocarcinoma cell line (CRL-2119) in DMEM-F12. The Raji CD19KO cell line was derived from original Raji cells by targeting the first exon of the *CD19* gene using clustered regularly interspaced short palindromic repeats (CRISPR)/Cas9 technology, as described by Ran et al.<sup>64</sup> Cell culture media (Sigma-Aldrich) were supplemented with 5%–20% heat-inactivated fetal calf serum (Invitrogen) and 2 mM L-glutamine (Sigma-Aldrich). OVCAR3 and HPAC cell culture media were additionally supplemented with 10 mM 4-(2-hydroxyethyl)-1-piperazineethanesulfonic acid (HEPES), 1 mM sodium pyruvate (Sigma-Aldrich), and insulin

transferring selenium ethanolamine (ITS) (Invitrogen). HPAC cell culture medium also contained 10 ng/ml epidermal growth factor (Invitrogen) and 40 ng/ml hydrocortisone (Sigma-Aldrich). Cells were cultured at 37°C and 5% CO<sub>2</sub>.

Clinical-grade rituximab (anti-CD20 human IgG1 antibody) was obtained from FarmaMondo. The anti-mesothelin monoclonal antibody amatuximab (MORAb-009, Morphotek/Eisai) was cloned (PDB: 4F3F\_A and 4F3F\_B) and expressed as human IgG1 in Chinese hamster ovary (CHO) cells. The hybridoma-expressing mouse anti-human CD47 blocking mAb B6H12<sup>52</sup> was purchased from the ATCC (clone B6H12.2, HB-9771). The mAb B6H12 was either produced and purified directly from hybridoma supernatants in its native form (mouse IgG1) or cloned and expressed as human IgG1 in CHO cells (mAb B6H12-hIgG1). The latter form was used in whole-blood binding experiments (Figure 6; Figures S7 and S8).

### Flow Cytometry

To assess antibody selectivity, TAA-positive cells (Raji or NCI-N87) were stained with 0.2  $\mu$ M carboxyfluorescein diacetate succinimidyl ester (CFSE) (Invitrogen), mixed with unstained TAA-negative cells (RAJI CD19KO or A-431) in a 1:1 ratio, and incubated ( $2.0 \times 10^5$  cells/well) with 0.1  $\mu$ g/mL of biAb for 30 min at 4°C in fluorescence-activated cell sorting (FACS) buffer (PBS, 2% BSA, and 0.1% NaN<sub>3</sub>) supplemented with 10% mouse serum (Sigma-Aldrich). BiAb-bound cells were then washed and stained for 15 min at 4°C with phycoerythrin (PE)-mouse anti-human Fc secondary antibody (clone H2, Southern Biotech). Propidium iodide (Sigma-Aldrich) was added before acquisition to exclude dead cells. Antibody binding to CFSE-labeled TAA-positive cells and unstained TAA-negative cells was measured by flow cytometry using a FACSCalibur flow cytometer (BD Biosciences) or a Cytoflex cytometer (Beckman Coulter). Results were analyzed using FlowJo software (Tree Star).

To compare binding of biAbs and monovalent control antibodies in dose-range experiments, increasing concentrations of test antibodies were incubated with double-positive cells ( $2.0 \times 10^5$ /well) in 96-well-plates for 30 min at 4°C in FACS buffer and analyzed as described above.

Quantification of cell surface receptor density was determined with QIFIKIT (Dako, K0078) according to the manufacturer's instructions. The following primary mouse mAb were used: anti-CD19 mAb4867 and anti-mesothelin mAb62653, both from R&D Systems, and the anti-CD47 mAb B6H12 produced at Novimmune.

Antibody binding in whole blood was determined as follows. Test antibody was pre-incubated with Alexa Fluor 647 polyclonal goat Fab-anti-human Fc (Jackson ImmunoResearch) at a 2:1 ratio for 15 min at 4°C to minimize background staining that may arise from free secondary/detection antibody being captured by cell surface and serum immunoglobulin. The antibody mixture was complemented with cell type-specific detection reagents such as PE mouse anti-CD235a (clone HIR2), PE mouse anti-CD41a (clone H1P8),

and fluorescein isothiocyanate (FITC) mouse anti-CD62P (clone AK4) from BD Biosciences or PE mouse anti-CD20 (clone HI47) from Thermo Fisher Scientific. The above antibodies bind specific cell populations in both human and cynomolgus blood (RBCs, platelets, and B cells, respectively). This antibody mixture (20× concentrated) was added to heparinized, EDTA-containing whole blood and incubated for 15 min at 4°C. For RBC binding, whole blood cells were washed and analyzed directly by flow cytometry. Analysis of B cell and platelet binding was done separately, after lysis of erythrocytes with BD FACS lysing solution as recommended by the manufacturer (BD Biosciences). Propidium iodide (Sigma-Aldrich) was added before acquisition to exclude dead cells.

### Phagocytosis Assay

Human peripheral blood mononuclear cells (PBMCs) were isolated from buffy coats by Ficoll gradient. Macrophages were generated by culturing PBMCs for 7 days in complete medium (RPMI 1640, 10% heat-inactivated fetal calf serum [Invitrogen]), 2 mM L-glutamine, 1 mM sodium pyruvate, 10 mM HEPES buffer, 25 µg/mL gentamicin (all from Sigma-Aldrich), and 50 µM 2-mercaptoethanol (Thermo Fisher Scientific) in the presence of 20 ng/mL of human macrophage colony-stimulating factor (M-CSF) (PeproTech). Non-adherent cells were subsequently eliminated by washes using PBS, and adherent cells representing macrophages were detached using cell dissociation buffer (Sigma-Aldrich) and washed in complete medium.

Target cells stained with 0.2 µM CFSE (Invitrogen) were incubated with antibody for 15 min at 37°C. For phagocytosis to proceed, macrophages were co-incubated with CFSE-labeled target cells and the antibody in ultra-low attachment 96-well plates (Corning) for 2.5 hr at 37°C. The quantity of cells per well and the effector/target (E/T) ratio varied between experiments. Typically, phagocytosis experiments with B cell leukemia/lymphoma cell lines were performed with  $5 \times 10^4$  macrophages and  $25 \times 10^4$  target cells per well (E/T ratio 1/5). Phagocytosis experiments with epithelial tumor cells were done with  $15 \times 10^4$  macrophages and  $5 \times 10^4$  target cells per well (E/T ratio 3/1) unless indicated otherwise. After completion of phagocytosis, macrophages were labeled by addition of allophycocyanin (APC)-labeled mouse anti-CD14 antibody (clone M5E2, BD Biosciences). Cells were then washed, and 7-aminoactinomycin D was added to identify dead cells (eBioscience). Phagocytosis was quantified by three-color flow cytometry. CD14+ CFSE+ double-positive events were identified as phagocytosis. The calculation of the percentage of phagocytosis varied depending on the E/T ratio. The percentage of phagocytosis is either presented as the ratio between CD14+ CFSE+ double-positive and total macrophages  $\times 100$  (E/T ratio 1/5) or as the ratio between CD14+ CFSE+ double-positive and total target cells  $\times 100$  (E/T ratio 3/1).

For phagocytosis performed in the presence of RBCs, erythrocytes were isolated from human whole blood by centrifugation at  $450 \times g$ , washed three times in PBS, and pre-incubated with macrophages in the presence of the test antibody for 15 min at 37°C before the addition of CFSE-labeled target cells. Phagocytosis and FACS analysis were

done as described above, except that the erythrocytes were lysed with FACS lysing solution before macrophage staining.

### In Vivo Xenograft Model

All animal experiments were performed in accordance with the Swiss animal protection law and institutional animal guidelines.  $2 \times 10^6$  Raji cells were injected subcutaneously into the flank of 6- to 10-week-old NOD/SCID mice (Charles River Laboratories). Tumor volume was measured using a caliper and calculated using the formula (width  $\times$  length  $\times$  height  $\times$  Pi)/6. Treatment was initiated when the tumor reached about 200 mm<sup>3</sup>. Mice received doses of 400 µg therapeutic antibody by intraperitoneal administration three times per week during 3 weeks. Animals were euthanized when the tumor volume exceeded 1,500 mm<sup>3</sup> or at the endpoint (28 days following start of treatment).

### Pharmacokinetics and Tolerability Assessment

A single-dose pharmacokinetics study was performed in cynomolgus monkeys at the Covance Laboratories test facility. All procedures in the study were in compliance with the German Animal Welfare Act and were approved by the local Institutional Animal Care and Use Committee. 2- to 3-year-old females (n = 3/dose group) were injected by intravenous bolus with either 0.5 mg/kg or 10 mg/kg of the anti-CD47/CD19 biAb. The animals were assessed twice daily for clinical symptoms. Blood samples were collected prior to dosing and at different time points post-dosing for a period of 8 weeks for hematological and pharmacokinetic analyses. Macroscopic examinations were performed on all organs/tissues at necropsy. biAb serum concentrations were measured by ELISA at Novimmune with an immunoassay specific for human IgG. The evaluation of the pharmacokinetics data was conducted at Novimmune using a pharmacokinetic software package (WinNonlin Professional Version 6.3, Pharsight).

### SUPPLEMENTAL INFORMATION

Supplemental Information includes Supplemental Materials and Methods, nine figures, and one table and can be found with this article online at <http://dx.doi.org/10.1016/j.ymthe.2016.11.006>.

### AUTHOR CONTRIBUTIONS

Conceptualization, F.R., M.K.V., N.F., and K.M.; Methodology, E.D., V.M., L.B., A.P., S.S.P., S.M., R.N., and K.M.; Investigation, E.D., V.M., L.B., A.P., L.C., S.C., and S.M.; Formal Analysis, E.D. S.S.P., and Z.J.; Writing – Original Draft, E.D. and K.M.; Writing – Review & Editing: E.D., S.S.P., Z.J., S.M., R.N., F.R., W.F., M.K.V., N.F., and K.M.; Supervision, V.M., S.S.P., Z.J., R.N., W.F., M.K.V., N.F., and K.M.

### CONFLICTS OF INTEREST

The authors are current or former employees of Novimmune SA. The authors declare no competing financial interests.

### ACKNOWLEDGMENTS

We thank G. Magistrelli, Y. Poitevin, G. Pontini, P. Malinge, and S. Jossier for help with antibody expression and purification; U.

Ravn, F. Gueneau, N. Bosson, N. Costes, M. Charreton-Galby, and M. Guerrier for library construction and phage display sections; L. Barba and E. Escoffier for skillful technical assistance; and G. Didelot for the CD19KO cell line.

## REFERENCES

- Sharma, P., and Allison, J.P. (2015). The future of immune checkpoint therapy. *Science* 348, 56–61.
- Pardoll, D.M. (2012). The blockade of immune checkpoints in cancer immunotherapy. *Nat. Rev. Cancer* 12, 252–264.
- Palucka, A.K., and Coussens, L.M. (2016). The Basis of Oncoimmunology. *Cell* 164, 1233–1247.
- Melero, I., Berman, D.M., Aznar, M.A., Korman, A.J., Pérez Gracia, J.L., and Haanen, J. (2015). Evolving synergistic combinations of targeted immunotherapies to combat cancer. *Nat. Rev. Cancer* 15, 457–472.
- Mills, C.D., Lenz, L.L., and Harris, R.A. (2016). A Breakthrough: Macrophage-Directed Cancer Immunotherapy. *Cancer Res.* 76, 513–516.
- Weiskopf, K., and Weissman, I.L. (2015). Macrophages are critical effectors of antibody therapies for cancer. *Mabs* 7, 303–310.
- Oldenborg, P.A., Zheleznyak, A., Fang, Y.F., Lagenaur, C.F., Gresham, H.D., and Lindberg, F.P. (2000). Role of CD47 as a marker of self on red blood cells. *Science* 288, 2051–2054.
- Brown, E.J., and Frazier, W.A. (2001). Integrin-associated protein (CD47) and its ligands. *Trends Cell Biol.* 11, 130–135.
- Jaiswal, S., Jamieson, C.H., Pang, W.W., Park, C.Y., Chao, M.P., Majeti, R., Traver, D., van Rooijen, N., and Weissman, I.L. (2009). CD47 is upregulated on circulating hematopoietic stem cells and leukemia cells to avoid phagocytosis. *Cell* 138, 271–285.
- Majeti, R., Chao, M.P., Alizadeh, A.A., Pang, W.W., Jaiswal, S., Gibbs, K.D., Jr., van Rooijen, N., and Weissman, I.L. (2009). CD47 is an adverse prognostic factor and therapeutic antibody target on human acute myeloid leukemia stem cells. *Cell* 138, 286–299.
- Tsai, R.K., and Discher, D.E. (2008). Inhibition of “self” engulfment through deactivation of myosin-II at the phagocytic synapse between human cells. *J. Cell Biol.* 180, 989–1003.
- Oldenborg, P.A., Gresham, H.D., and Lindberg, F.P. (2001). CD47-signal regulatory protein alpha (SIRPalpha) regulates Fcgamma and complement receptor-mediated phagocytosis. *J. Exp. Med.* 193, 855–862.
- Gardai, S.J., McPhillips, K.A., Frasch, S.C., Janssen, W.J., Starefeldt, A., Murphy-Ullrich, J.E., Bratton, D.L., Oldenborg, P.A., Michalak, M., and Henson, P.M. (2005). Cell-surface calreticulin initiates clearance of viable or apoptotic cells through trans-activation of LRP on the phagocyte. *Cell* 123, 321–334.
- Chao, M.P., Weissman, I.L., and Majeti, R. (2012). The CD47-SIRPα pathway in cancer immune evasion and potential therapeutic implications. *Curr. Opin. Immunol.* 24, 225–232.
- Baccelli, I., Stenzinger, A., Vogel, V., Pfltzner, B.M., Klein, C., Wallwiener, M., Scharpf, M., Saini, M., Holland-Letz, T., Sinn, H.P., et al. (2014). Co-expression of MET and CD47 is a novel prognosticator for survival of luminal breast cancer patients. *Oncotarget* 5, 8147–8160.
- Baccelli, I., Schneeweiss, A., Riethdorf, S., Stenzinger, A., Schillert, A., Vogel, V., Klein, C., Saini, M., Bäuerle, T., Wallwiener, M., et al. (2013). Identification of a population of blood circulating tumor cells from breast cancer patients that initiates metastasis in a xenograft assay. *Nat. Biotechnol.* 31, 539–544.
- Chan, K.S., Espinosa, I., Chao, M., Wong, D., Ailles, L., Diehn, M., Gill, H., Presti, J., Jr., Chang, H.Y., van de Rijn, M., et al. (2009). Identification, molecular characterization, clinical prognosis, and therapeutic targeting of human bladder tumor-initiating cells. *Proc. Natl. Acad. Sci. USA* 106, 14016–14021.
- Cioffi, M., Trabulo, S., Hidalgo, M., Costello, E., Greenhalf, W., Erkan, M., Kleeff, J., Sainz, B., Jr., and Heeschen, C. (2015). Inhibition of CD47 effectively targets pancreatic cancer stem cells via dual mechanisms. *Clin. Cancer Res.* 21, 2325–2337.
- Lee, T.K., Cheung, V.C., Lu, P., Lau, E.Y., Ma, S., Tang, K.H., Tong, M., Lo, J., and Ng, I.O. (2014). Blockade of CD47-mediated cathepsin S/protease-activated receptor 2 signaling provides a therapeutic target for hepatocellular carcinoma. *Hepatology* 60, 179–191.
- Willingham, S.B., Volkmer, J.P., Gentles, A.J., Sahoo, D., Dalerba, P., Mitra, S.S., Wang, J., Contreras-Trujillo, H., Martin, R., Cohen, J.D., et al. (2012). The CD47-signal regulatory protein alpha (SIRPα) interaction is a therapeutic target for human solid tumors. *Proc. Natl. Acad. Sci. USA* 109, 6662–6667.
- Chao, M.P., Alizadeh, A.A., Tang, C., Myklebust, J.H., Varghese, B., Gill, S., Jan, M., Cha, A.C., Chan, C.K., Tan, B.T., et al. (2010). Anti-CD47 antibody synergizes with rituximab to promote phagocytosis and eradicate non-Hodgkin lymphoma. *Cell* 142, 699–713.
- Wang, H., Tan, M., Zhang, S., Li, X., Gao, J., Zhang, D., Hao, Y., Gao, S., Liu, J., and Lin, B. (2015). Expression and significance of CD44, CD47 and c-met in ovarian clear cell carcinoma. *Int. J. Mol. Sci.* 16, 3391–3404.
- Xiao, Z., Chung, H., Banan, B., Manning, P.T., Ott, K.C., Lin, S., Capoccia, B.J., Subramanian, V., Hiebsch, R.R., Upadhyaya, G.A., et al. (2015). Antibody mediated therapy targeting CD47 inhibits tumor progression of hepatocellular carcinoma. *Cancer Lett.* 360, 302–309.
- Yoshida, K., Tsujimoto, H., Matsumura, K., Kinoshita, M., Takahata, R., Matsumoto, Y., Hiraki, S., Ono, S., Seki, S., Yamamoto, J., and Hase, K. (2015). CD47 is an adverse prognostic factor and a therapeutic target in gastric cancer. *Cancer Med.* 4, 1322–1333.
- Weiskopf, K., Ring, A.M., Ho, C.C., Volkmer, J.P., Levin, A.M., Volkmer, A.K., Ozkan, E., Fernhoff, N.B., van de Rijn, M., Weissman, I.L., and Garcia, K.C. (2013). Engineered SIRPα variants as immunotherapeutic adjuvants to anticancer antibodies. *Science* 341, 88–91.
- Zhao, X.W., van Beek, E.M., Schornagel, K., Van der Maaden, H., Van Houdt, M., Otten, M.A., Finetti, P., Van Egmond, M., Matozaki, T., Kraal, G., et al. (2011). CD47-signal regulatory protein-α (SIRPα) interactions form a barrier for antibody-mediated tumor cell destruction. *Proc. Natl. Acad. Sci. USA* 108, 18342–18347.
- Edris, B., Weiskopf, K., Volkmer, A.K., Volkmer, J.P., Willingham, S.B., Contreras-Trujillo, H., Liu, J., Majeti, R., West, R.B., Fletcher, J.A., et al. (2012). Antibody therapy targeting the CD47 protein is effective in a model of aggressive metastatic leiomyosarcoma. *Proc. Natl. Acad. Sci. USA* 109, 6656–6661.
- Lo, J., Lau, E.Y., So, F.T., Lu, P., Chan, V.S., Cheung, V.C., Ching, R.H., Cheng, B.Y., Ma, M.K., Ng, I.O., and Lee, T.K. (2016). Anti-CD47 antibody suppresses tumour growth and augments the effect of chemotherapy treatment in hepatocellular carcinoma. *Liver Int.* 36, 737–745.
- Sagawa, M., Shimizu, T., Fukushima, N., Kinoshita, Y., Ohizumi, I., Uno, S., Kikuchi, Y., Ikeda, Y., Yamada-Okabe, H., and Kizaki, M. (2011). A new disulfide-linked dimer of a single-chain antibody fragment against human CD47 induces apoptosis in lymphoid malignant cells via the hypoxia inducible factor-1α pathway. *Cancer Sci.* 102, 1208–1215.
- Uno, S., Kinoshita, Y., Azuma, Y., Tsunenari, T., Yoshimura, Y., Iida, S., Kikuchi, Y., Yamada-Okabe, H., and Fukushima, N. (2007). Antitumor activity of a monoclonal antibody against CD47 in xenograft models of human leukemia. *Oncol. Rep.* 17, 1189–1194.
- Mateo, V., Lagneaux, L., Bron, D., Biron, G., Armant, M., Delespese, G., and Sarfati, M. (1999). CD47 ligation induces caspase-independent cell death in chronic lymphocytic leukemia. *Nat. Med.* 5, 1277–1284.
- Zhang, H., Lu, H., Xiang, L., Bullen, J.W., Zhang, C., Samanta, D., Gilkes, D.M., He, J., and Semenza, G.L. (2015). HIF-1 regulates CD47 expression in breast cancer cells to promote evasion of phagocytosis and maintenance of cancer stem cells. *Proc. Natl. Acad. Sci. USA* 112, E6215–E6223.
- Kaur, S., Elkahoul, A.G., Singh, S.P., Chen, Q.R., Meerzaman, D.M., Song, T., Manu, N., Wu, W., Mannan, P., Garfield, S.H., and Roberts, D.D. (2016). A function-blocking CD47 antibody suppresses stem cell and EGF signaling in triple-negative breast cancer. *Oncotarget* 7, 10133–10152.
- Soto-Pantoja, D.R., Terabe, M., Ghosh, A., Ridnour, L.A., DeGraff, W.G., Wink, D.A., Berzofsky, J.A., and Roberts, D.D. (2014). CD47 in the tumor microenvironment limits cooperation between antitumor T-cell immunity and radiotherapy. *Cancer Res.* 74, 6771–6783.

35. Liu, X., Pu, Y., Cron, K., Deng, L., Kline, J., Frazier, W.A., Xu, H., Peng, H., Fu, Y.X., and Xu, M.M. (2015). CD47 blockade triggers T cell-mediated destruction of immunogenic tumors. *Nat. Med.* *21*, 1209–1215.
36. Wang, Y., Xu, Z., Guo, S., Zhang, L., Sharma, A., Robertson, G.P., and Huang, L. (2013). Intravenous delivery of siRNA targeting CD47 effectively inhibits melanoma tumor growth and lung metastasis. *Mol. Ther.* *21*, 1919–1929.
37. Sockolovsky, J.T., Dougan, M., Ingram, J.R., Ho, C.C., Kauke, M.J., Almo, S.C., Ploegh, H.L., and Garcia, K.C. (2016). Durable antitumor responses to CD47 blockade require adaptive immune stimulation. *Proc. Natl. Acad. Sci. USA* *113*, E2646–E2654.
38. Tseng, D., Volkmer, J.P., Willingham, S.B., Contreras-Trujillo, H., Fathman, J.W., Fernhoff, N.B., Seita, J., Inlay, M.A., Weiskopf, K., Miyanishi, M., and Weissman, I.L. (2013). Anti-CD47 antibody-mediated phagocytosis of cancer by macrophages primes an effective antitumor T-cell response. *Proc. Natl. Acad. Sci. USA* *110*, 11103–11108.
39. Liu, J., Wang, L., Zhao, F., Tseng, S., Narayanan, C., Shura, L., Willingham, S., Howard, M., Prohaska, S., Volkmer, J., et al. (2015). Pre-Clinical Development of a Humanized Anti-CD47 Antibody with Anti-Cancer Therapeutic Potential. *PLoS ONE* *10*, e0137345.
40. Ho, C.C., Guo, N., Sockolovsky, J.T., Ring, A.M., Weiskopf, K., Özkan, E., Mori, Y., Weissman, I.L., and Garcia, K.C. (2015). “Velcro” engineering of high affinity CD47 ectodomain as signal regulatory protein  $\alpha$  (SIRP $\alpha$ ) antagonists that enhance antibody-dependent cellular phagocytosis. *J. Biol. Chem.* *290*, 12650–12663.
41. Kontermann, R.E., and Brinkmann, U. (2015). Bispecific antibodies. *Drug Discov. Today* *20*, 838–847.
42. Spiess, C., Zhai, Q., and Carter, P.J. (2015). Alternative molecular formats and therapeutic applications for bispecific antibodies. *Mol. Immunol.* *67* (2 Pt A), 95–106.
43. Chan, A.C., and Carter, P.J. (2010). Therapeutic antibodies for autoimmunity and inflammation. *Nat. Rev. Immunol.* *10*, 301–316.
44. Kontermann, R.E. (2012). Dual targeting strategies with bispecific antibodies. *MAbs* *4*, 182–197.
45. Piccione, E.C., Juarez, S., Liu, J., Tseng, S., Ryan, C.E., Narayanan, C., Wang, L., Weiskopf, K., and Majeti, R. (2015). A bispecific antibody targeting CD47 and CD20 selectively binds and eliminates dual antigen expressing lymphoma cells. *MAbs* *7*, 946–956.
46. Piccione, E.C., Juarez, S., Tseng, S., Liu, J., Stafford, M., Narayanan, C., Wang, L., Weiskopf, K., and Majeti, R. (2016). SIRP $\alpha$ -Antibody Fusion Proteins Selectively Bind and Eliminate Dual Antigen-Expressing Tumor Cells. *Clin. Cancer Res.* *22*, 5109–5119.
47. Pastan, I., and Hassan, R. (2014). Discovery of mesothelin and exploiting it as a target for immunotherapy. *Cancer Res.* *74*, 2907–2912.
48. Bournazos, S., and Ravetch, J.V. (2015). Fc $\gamma$  receptor pathways during active and passive immunization. *Immunol. Rev.* *268*, 88–103.
49. Nimmerjahn, F., and Ravetch, J.V. (2008). Fc $\gamma$  receptors as regulators of immune responses. *Nat. Rev. Immunol.* *8*, 34–47.
50. Jiang, X.R., Song, A., Bergelson, S., Arroll, T., Parekh, B., May, K., Chung, S., Strouse, R., Mire-Sluis, A., and Schenerman, M. (2011). Advances in the assessment and control of the effector functions of therapeutic antibodies. *Nat. Rev. Drug Discov.* *10*, 101–111.
51. Fischer, N., Elson, G., Magistrelli, G., Dheilly, E., Fouque, N., Laurendon, A., Gueneau, F., Ravn, U., Depoisier, J.F., Moine, V., et al. (2015). Exploiting light chains for the scalable generation and platform purification of native human bispecific IgG. *Nat. Commun.* *6*, 6113.
52. Gresham, H.D., Goodwin, J.L., Allen, P.M., Anderson, D.C., and Brown, E.J. (1989). A novel member of the integrin receptor family mediates Arg-Gly-Asp-stimulated neutrophil phagocytosis. *J. Cell Biol.* *108*, 1935–1943.
53. Gül, N., and van Egmond, M. (2015). Antibody-Dependent Phagocytosis of Tumor Cells by Macrophages: A Potent Effector Mechanism of Monoclonal Antibody Therapy of Cancer. *Cancer Res.* *75*, 5008–5013.
54. Leidi, M., Gotti, E., Bologna, L., Miranda, E., Rimoldi, M., Sica, A., Roncalli, M., Palumbo, G.A., Introna, M., and Golay, J. (2009). M2 macrophages phagocytose rituximab-opsonized leukemic targets more efficiently than m1 cells in vitro. *J. Immunol.* *182*, 4415–4422.
55. Subramanian, S., Tsai, R., Sen, S., Dahl, K.N., and Discher, D.E. (2006). Membrane mobility and clustering of Integrin Associated Protein (IAP, CD47)–major differences between mouse and man and implications for signaling. *Blood Cells Mol. Dis.* *36*, 364–372.
56. Mouro-Chanteloup, I., Delaunay, J., Gane, P., Nicolas, V., Johansen, M., Brown, E.J., Peters, L.L., Van Kim, C.L., Cartron, J.P., and Colin, Y. (2003). Evidence that the red cell skeleton protein 4.2 interacts with the Rh membrane complex member CD47. *Blood* *101*, 338–344.
57. Oldenburg, P.A. (2013). CD47: A Cell Surface Glycoprotein Which Regulates Multiple Functions of Hematopoietic Cells in Health and Disease. *ISRN Hematol.* *2013*, 614619.
58. Barclay, A.N., and Van den Berg, T.K. (2014). The interaction between signal regulatory protein alpha (SIRP $\alpha$ ) and CD47: structure, function, and therapeutic target. *Annu. Rev. Immunol.* *32*, 25–50.
59. Sick, E., Jeanne, A., Schneider, C., Dedieu, S., Takeda, K., and Martiny, L. (2012). CD47 update: a multifaceted actor in the tumour microenvironment of potential therapeutic interest. *Br. J. Pharmacol.* *167*, 1415–1430.
60. Soto-Pantoja, D.R., Kaur, S., and Roberts, D.D. (2015). CD47 signaling pathways controlling cellular differentiation and responses to stress. *Crit. Rev. Biochem. Mol. Biol.* *50*, 212–230.
61. Sarfati, M., Fortin, G., Raymond, M., and Susin, S. (2008). CD47 in the immune response: role of thrombospondin and SIRP-alpha reverse signaling. *Curr. Drug Targets* *9*, 842–850.
62. Murata, Y., Kotani, T., Ohnishi, H., and Matozaki, T. (2014). The CD47-SIRP $\alpha$  signalling system: its physiological roles and therapeutic application. *J. Biochem.* *155*, 335–344.
63. Matozaki, T., Murata, Y., Okazawa, H., and Ohnishi, H. (2009). Functions and molecular mechanisms of the CD47-SIRP $\alpha$  signalling pathway. *Trends Cell Biol.* *19*, 72–80.
64. Ran, F.A., Hsu, P.D., Wright, J., Agarwala, V., Scott, D.A., and Zhang, F. (2013). Genome engineering using the CRISPR-Cas9 system. *Nat. Protoc.* *8*, 2281–2308.